

Relative Energy and Structural Differences of Axial and Equatorial 1-Fluoro-1-silacyclohexane

Laura B. Favero,[†] Biagio Velino,[‡] Walther Caminati,^{*,§} Ingvar Árnason,[#] and Ágúst Kvaran[#]

Istituto per lo Studio dei Materiali Nanostrutturati (ISMN, Sezione di Bologna), CNR, Via Gobetti 101, I-40129 Bologna, Italy, Dipartimento di Chimica Fisica e Inorganica dell'Università, Viale Risorgimento 4, I-40136 Bologna, Italy, Dipartimento di Chimica "G. Ciamician" dell'Università, Via Selmi 2, I-40126 Bologna, Italy, and Science Institute, University of Iceland, Dunhaga 3, 107 Reykjavík, Iceland

Received: March 14, 2006; In Final Form: June 21, 2006

The rotational spectra of the main isotopomer, of the ²⁹Si and of all ¹³C isotopologues of axial and equatorial forms of 1-fluoro-silacyclohexane have been measured by conventional (only main species) and molecular beam Fourier transform microwave spectroscopy. *r*₀ and partial *r*_s structures are given separately for the two forms. The main structural differences are discussed. From dipole moments and relative intensity measurements, a slight preference ($E_{\text{Eq}} - E_{\text{Ax}} = 42 \pm 24 \text{ cm}^{-1}$) for the axial conformer was found. The rotational spectra of some, the most intense, vibrational satellites have also been measured. They belong to the ring-puckering motions.

Introduction

Equatorial–axial conformational equilibria and molecular structures of monosubstituted halo derivatives of cyclohexane have been investigated extensively.^{1–15} A general preference for the equatorial conformer is found.¹⁶ We believe that the more precise structural information and energy differences are those obtained by rotational spectroscopy.^{3,6,13}

Little is known experimentally about equatorial–axial conformational equilibria of monosubstituted derivatives of silacyclohexane. The rotational spectrum of silacyclohexane itself has been reported only very recently.¹⁷ The conformational equilibrium of 1-methyl-1-silacyclohexane has been investigated by gas-phase electron diffraction, low-temperature NMR, and quantum chemical calculations.¹⁸ No comparable data are available on halo derivatives of silacyclohexane. The covalent radii of C and Si (0.77 and 1.17 Å, respectively) and their electronic properties are considerably different. Therefore, a different behavior in the conformational equilibrium of the axial/equatorial form of 1-halo-1-silacyclohexanes, compared to the corresponding halocyclohexanes, could take place. For this reason we decided to investigate the rotational spectrum of the simplest member of the series, 1-fluoro-1-silacyclohexane (FSCH). The two conformers are shown in Table 1.

An analysis of the rotational spectra of some ring puckering satellite lines was also carried out, which provided information about the conformational interconversion barrier.

Experimental Methods

FSCH was prepared from 1-chloro-1-silacyclohexane by a treatment with 40% aqueous HF according to a general literature method.¹⁹ A more detailed procedure will be given elsewhere.²⁰

* Corresponding author. Fax: +39 051 2099456. Tel: +39 051 2099480. E-mail: walther.caminati@unibo.it.

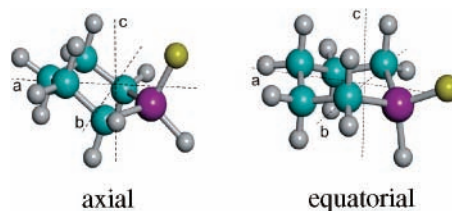
[†] Istituto per lo Studio dei Materiali Nanostrutturati.

[‡] Dipartimento di Chimica Fisica e Inorganica dell'Università.

[§] Dipartimento di Chimica "G. Ciamician" dell'Università.

[#] University of Iceland.

TABLE 1: Ab Initio Spectroscopic Parameters of FSCH, Obtained at the MP2/6-311++G** Level of Theory



	axial	equatorial
<i>A</i> /MHz	2967.3	3525.0
<i>B</i> /MHz	1917.7	1685.2
<i>C</i> /MHz	1494.5	1261.9
μ_a/D^a	1.65	2.28
μ_c/D	1.32	−0.20
$\Delta E/cm^{-1}$	0	80

^a $\mu_b = 0$ by symmetry.

Two microwave (MW) techniques have been used. They are described as follows:

(a) MW spectra in a standing waveguide cell were recorded in the frequency range 26.5–39.6 GHz with a computer controlled Stark spectrometer based on a Hewlett-Packard 8400 C instrument. The radio frequency-microwave double resonance (rfmwdr) technique²¹ was used for the assignment of the first transitions. The absorption cell temperature was kept constant at about −20 °C. The accuracy of the frequency measurements is about 0.05 MHz.

(b) The spectrum in the 6–18 GHz frequency region was measured using the COBRA-type²² molecular beam Fourier transform MW (MB-FTMW) spectrometer described elsewhere.²³ Argon at a pressure of 2.5 bar was flown over liquid FSCH at room temperature, and expanded through the solenoid valve (General Valve, Series 9, nozzle diameter 0.5 mm) into the Fabry–Pérot cavity. The frequencies were determined after Fourier transformation of the 8k data points time domain signal, recorded with 100 ns sample intervals. The rest frequencies of each rotational transition were calculated as the arithmetic mean

TABLE 2: Spectroscopic Constants (A Reduction, I^r Representation) of the Ground States of the Main Species and of Several Isotopologues of Axial and Equatorial FSCH

	main	²⁹ Si	³⁰ Si	¹³ C2	¹³ C3	¹³ C4
			Axial			
<i>A</i> /MHz	2988.1146(1) ^a	2984.3780(5)	2980.7709(5)	2944.9404(9)	2957.3379(6)	2988.1335(7)
<i>B</i> /MHz	1935.4401(5)	1925.4339(3)	1915.7156(3)	1933.4246(6)	1922.4567(4)	1904.9004(4)
<i>C</i> /MHz	1502.1986(4)	1497.1166(2)	1492.1508(5)	1492.4966(3)	1487.8205(2)	1483.7910(3)
Δ_J /kHz	0.522(4)	[0.522] ^b	[0.522] ^b	[0.522]	[0.522]	[0.522]
Δ_{JK} /kHz	-1.21(2)	[-1.21]	[-1.21]	[-1.21]	[-1.21]	[-1.21]
Δ_K /kHz	1.53(3)	[1.53]	[1.53]	[1.53]	[1.53]	[1.53]
δ_J /kHz	0.053(3)	[0.053]	[0.053]	[0.053]	[0.053]	[0.053]
δ_K /kHz	0.13(3)	[0.13]	[0.13]	[0.13]	[0.13]	[0.13]
<i>N</i> ^c	64	8	9	8	7	10
$\sigma/\sigma_{\text{exp}}$ ^d	1.2	0.6	0.6	0.9	0.6	0.6
			Equatorial			
<i>A</i> /MHz	3530.668(3)	3527.655(4)	3524.719(6)	3476.843(4)	3490.16(1)	3527.49(1)
<i>B</i> /MHz	1707.0771(5)	1701.1399(2)	1695.3535(4)	1706.9275(2)	1693.8659(4)	1680.9280(4)
<i>C</i> /MHz	1273.7435(5)	1270.8323(2)	1267.9869(4)	1266.8101(2)	1261.3500(4)	1259.5762(4)
Δ_J /kHz ^e	0.100(2) ^c	[0.100]	[0.100]	[0.100]	[0.100]	[0.100]
Δ_{JK} /kHz	0.055(8)	[0.055]	[0.055]	[0.055]	[0.055]	[0.055]
δ_J /kHz	0.022(2)	[0.022]	[0.022]	[0.022]	[0.022]	[0.022]
<i>N</i> ^c	75	5	9	6	5	8
$\sigma/\sigma_{\text{exp}}$ ^d	1.1	0.4	0.4	0.3	0.7	0.7

^a Error (in parentheses) is expressed in units of the last digit. ^b Centrifugal distortion parameters in brackets have been fixed to the values of the corresponding most abundant species. ^c Number of transitions in the fit. ^d Reduced deviation of the fit, relative to measurement errors of 3 and 50 kHz for the MW-FT and conventional spectrometer, respectively. ^e Centrifugal distortion parameters Δ_K and δ_K of the equatorial species have been fixed to zero because they are undetermined in the fit.

of the frequencies of the two Doppler components. The estimated accuracy of frequency measurements is better than 3 kHz. Lines separated by more than 7 kHz were resolvable..

Results and Discussion

(1) Theoretical Calculations. To estimate starting values for energies, rotational constants and dipole moment components of the axial and equatorial conformers, we performed theoretical calculations at the MP2/6-311++G** level of theory.²⁴ The results are reported in Table 1, together with the sketches of the two forms. Surprisingly, the axial conformer was calculated to be more stable.

(2) Rotational Spectrum. Trial calculations of the spectrum were based on the theoretical rotational constants mentioned above. The spectra of the two conformers, including those of some vibrational satellites, recorded with the standard cell Stark modulated spectrometer were assigned with the help of the rfmwdr technique. The assignment of the spectrum started by applying the rfmwdr technique to asymmetry doublet transitions with $K_a = 6$. The twin transitions $10_{6,5} \leftarrow 9_{6,4}$ and $10_{6,4} \leftarrow 9_{6,3}$, separated by 4.0 MHz, and $9_{6,4} \leftarrow 8_{6,3}$ and $9_{6,3} \leftarrow 8_{6,2}$, separated by 11.0 MHz, were assigned initially for the equatorial and axial species, respectively. Later, more transitions were measured, with either the rfmwdr or the Stark modulation technique. The frequencies are given as Supporting Information. At the same time we measured several more lines for the main species with the MB-FTMW spectrometer. Its unrivalled sensitivity allowed measurements and assignment of the spectra of five less abundant isotopologues (²⁹Si, ³⁰Si and all monosubstituted ¹³C species) in natural abundance. The MB-FTMW measured lines are also given as Supporting Information. The experimental frequencies were fitted with the I^r representation and *A* reduction of Watson's quartic Hamiltonian.²⁵ The spectroscopic constants of the ground states and of the vibrational satellites are reported in Tables 2 and 3, respectively.

(3) Structures of the two Conformers. From the available rotational constants, eighteen for each conformer, it is possible to obtain two kind of structural information. The r_s coordinates are the *a*, *b* and *c* coordinates of an atom in the principal axes

TABLE 3: Spectroscopic Constants (A-reduction, I^r Representation) Vibrational Energies and Shifts of Planar Moments of Inertia with Respect to the Corresponding Ground State of Three Vibrational Satellites of Axial and Equatorial FSCH^a

	axial			equatorial		
	$v = 1$	$v_1 = 1$	$v_2 = 1$			
<i>A</i> /MHz	2991.21(3)	3515.61(3)	3532.53(3)			
<i>B</i> /MHz	1933.684(3)	1708.554(1)	1706.862(1)			
<i>C</i> /MHz	1499.496(2)	1275.047(1)	1272.533(1)			
σ^b /MHz	0.08	0.09	0.06			
<i>N</i> ^c	22	46	33			
$E_{\text{vib}}^d/\text{cm}^{-1}$	110(30)	80(20)	170(10)			
$\Delta P_{aa}/\text{u}\text{\AA}^2$	0.510	-0.636	0.243			
$\Delta P_{bb}/\text{u}\text{\AA}^2$	0.100	0.234	0.133			
$\Delta P_{cc}/\text{u}\text{\AA}^2$	-0.269	0.378	-0.205			

^a Centrifugal distortion constants fixed at the values of the corresponding ground states. ^b Standard deviation of the fit. ^c Number of transitions of the fit. ^d From relative intensity measurements.

system of the main species. Their absolute values are easily obtained when the spectrum of the corresponding singly isotopic substituted species is available.²⁶ The r_0 geometries are determined by fitting the rotational constants of the ground states and therefore supply the molecular structures averaged over the vibrational ground states wave functions. The r_s structure is thought to be intermediate between the r_0 and the r_e (*e* is for equilibrium, relative to a hypothetical vibrationless molecule) structure, because the vibrational effects are more less the same for the main and for the isotopically substituted species.

The substitution coordinates of atoms Si, C2, C3 and C4, are reported in Table 4. The $|a|$ coordinate of C2 and the $|b|$ coordinates of C4 and Si *a*-coordinate do have small, physically insignificant, imaginary values. This is within the limitations that underline the Kraitchman procedure.²⁶ We could, however, obtain from them some approximated r_s structural parameters (listed in Table 5 together with the r_0 data) by fixing to zero the small imaginary values.

From the fit of the eighteen rotational constants, we could determine nine r_0 structural parameters for each conformer. Due to the symmetry of the molecule, they are sufficient to extract

TABLE 4: Substitution Coordinates (Å) of the Si, C2 and C3 Atoms of Axial and Equatorial FSCH

		axial				equatorial			
		Si ^a	C2	C3	C4	Si ^a	C2	C3	C4
a	exptl	1.073(3)	0.10 ^b	1.267(1)	2.015(7)	0.958(2)	0.10i(1) ^a	1.503(1)	2.1207(7)
	calc ^c	1.070	0.076	1.246	2.033	0.950	0.029	1.503	2.091
b	exptl	0.04 ^b	1.483(1)	1.288(1)	0.08 ^b	0.03 ^b	1.480(1)	1.287(1)	0.08 ^b
	calc ^c	0.0	1.491	1.282	0.0	0.0	1.482	1.289	0.0
c	exptl	0.466(3)	0.540(3)	0.376(4)	0.08(2)	0.353(4)	0.190(8)	0.193(8)	0.374(4)
	calc ^c	0.477	0.529	0.445	0.185	0.358	0.190	0.192	0.364

^a From the ²⁹Si species. ^b Imaginary value. ^c Calculated values with the partial *r*₀ geometry of Table 5.

TABLE 5: *r*₀, *r*_s and *r*_e Structures of Axial and Equatorial FSCH

	axial			equatorial		
	<i>r</i> ₀ ^a	<i>r</i> _s ^b	<i>r</i> _e ^c	<i>r</i> ₀ ^a	<i>r</i> _s ^b	<i>r</i> _e ^c
α	121.4(4)		121.4	126.4(2)		126.4
β	140.2(4)		139.7	136.2(2)		136.2
γ	122.0(5)		121.9	122.4(3)		122.3
<i>r</i> _{a-Si}	1.121(6)		1.125	1.222(6)		1.132
<i>r</i> _{b-C4}	0.828(10)		0.837	0.828(6)		0.835
<i>r</i> _{a-C2}	1.491(2)		1.489	1.482(1)		1.484
<i>r</i> _{b-C3}	1.282(2)		1.288	1.289(1)		1.288
<i>r</i> _{a-b}	1.523(7)		1.531	1.523(5)		1.534
F-Si	1.620(7)		1.637	1.624(7)		1.633
Si-C2	1.866(4) ^d	1.832	1.866	1.859(4)	1.845	1.866
C2-C3	1.537(7) ^d	1.576	1.544	1.535(6)	1.563	1.546
C3-C4	1.526(6) ^d	1.536	1.536	1.532(3)	1.519	1.535
C2-Si-C6	106.1(3) ^d	108.1	105.9	105.7(3)	106.6	105.3
Si-C2-C3	110.4(5) ^d	110.3	110.6	109.4(4)	109.2	109.5
C3-C4-C5	114.3(4) ^d	116.0	114.0	114.6(4)	114.1	114.1

^a See Figure 1 for the definition of α, β, γ and of the a and b intersection points. ^b *r*_s values have been calculated by fixing to zero the |a| coordinate of C2 and |b| coordinates of C4 and Si. ^c MP2/6-311++G** calculations. ^d Derived parameters, not required in the *r*₀ fit.

the structure of the seven heavy atoms frame. In the fit, we allowed these parameters to change, with respect to the ab initio values, in “confidence intervals”²⁷ of 0.01 Å for the bond distances and of 2° for the valence angles, respectively. It was necessary to keep the structural parameters of the hydrogen atoms fixed to the ab initio values (given in Table 6).

This assumption should have little effect on the heavy atoms structural parameters, because the inertial effects of the light hydrogen atoms are minor. The determined parameters, α, β, γ, *r*_{Si-F}, *r*_{ab}, *r*_{a-C2}, *r*_{b-C3}, *r*_{a-Si}, and *r*_{b-C4} (see Figure 1), are listed in Table 5. From these it was easy to derive more common parameters such as the C-C and C-Si bond lengths. For comparison, the ab initio geometries are also reported.

(4) Dipole Moment. The dipole moments of the axial and equatorial FSCH have been determined from the analysis of the second-order Stark effect on three and four transitions of the axial and equatorial species, respectively. A dc voltage has been added to the square wave modulation. The cell was calibrated with the 3 ← 2 transition of OCS (*μ* = 0.71521 D²⁸). The values Δ*ν*/*E*² for the observed Stark lobes are reported in

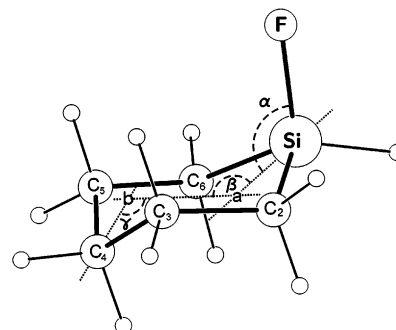


Figure 1. Structural parameters and symbols for FSCH used throughout the text. *a* and *b* are intersection points between the bisector of the C2SiC6 angle and the C2C6 line, and the bisector of the C3C4C5 angle and the C3C5 line, respectively. They lie in the plane of symmetry of the molecule.

Table 7, along with the results of a least-squares fit. The Stark coefficients²⁹ were calculated using the effective rotational constants in Table 2. One can see, by comparing the experimental dipole moments to the ab initio ones of Table 1, that the theoretical values are overestimated by about a 15%.

(5) Conformational Energies. The *μ*_a rotational transitions of the axial conformer appeared, at a first glance, equally strong as those of the equatorial one. An example is shown in Figure 2. We made more precise intensity measurements³⁰ of five pairs of *μ*_a-type rotational transitions (11_{1,10} ← 10_{1,9}, 11_{2,9} ← 10_{2,8}, 11_{2,10} ← 10_{2,9}, 10_{3,7} ← 9_{3,6} and 11_{3,9} ← 10_{3,8}) and determined their energy difference, according to the following equation:

$$E_{\text{Eq}} - E_{\text{Ax}} = kT \ln \left[\frac{(I_{\text{Ax}} \Delta \nu_{\text{Ax}} \mu_{\text{a,Ax}}^2 u_{\text{a,Eq}}^2 \nu_{\text{Eq}}^2)}{(I_{\text{Eq}} \Delta \nu_{\text{Eq}} \mu_{\text{a,Ax}}^2 u_{\text{a,Ax}}^2 \nu_{\text{Ax}}^2)} \right] \quad (1)$$

where *I* and Δ*ν* are the peak height and line width, respectively, *μ*_a is the dipole moment component, γ and *ν* are the line strength and frequency, respectively. In equation 1 we used the dipole moment components of Table 7, to obtain *E*_{Eq} - *E*_{Ax} = 42(24) cm⁻¹. This value is in agreement with that predicted by ab initio calculations (see Table 1).

These results outline that the axial/equatorial conformational behavior of FSCH is different with respect to that of the corresponding cyclohexane derivative:³ FSCH shows a slight preference for the axial conformer.

TABLE 6: Structural Parameters (Relative to Figure 1) of the Hydrogen Fixed at the MP2/6-311++G Values**

	bond lengths (Å)		valence angles (deg)				dihedral angles (deg)	
	axial	equat	axial	equat	axial	equat	axial	equat
Si-H	1.477	1.479	<i>a</i> -Si-H	132.4	127.1	C4-C3-C2-H _{eq}	-178.8	-179.6
C2-H _{eq}	1.096	1.096	Si-C2-H _{eq}	111.4	112.0	C4-C3-C2-H _{ax}	64.3	62.5
C2-H _{ax}	1.100	1.098	Si-C2-H _{ax}	108.4	108.8	Si-C2-C3-H _{eq}	-176.8	-178.5
C3-H _{eq}	1.096	1.096	C4-C3-H _{eq}	109.1	109.2	Si-C2-C3-H _{ax}	66.7	65.2
C3-H _{ax}	1.098	1.099	C4-C3-H _{ax}	108.6	108.7			
C4-H _{eq}	1.096	1.097	<i>b</i> -C4-H _{eq}	126.0	126.3			
C4-H _{ax}	1.100	1.099	<i>b</i> -C4-H _{ax}	127.3	127.0			

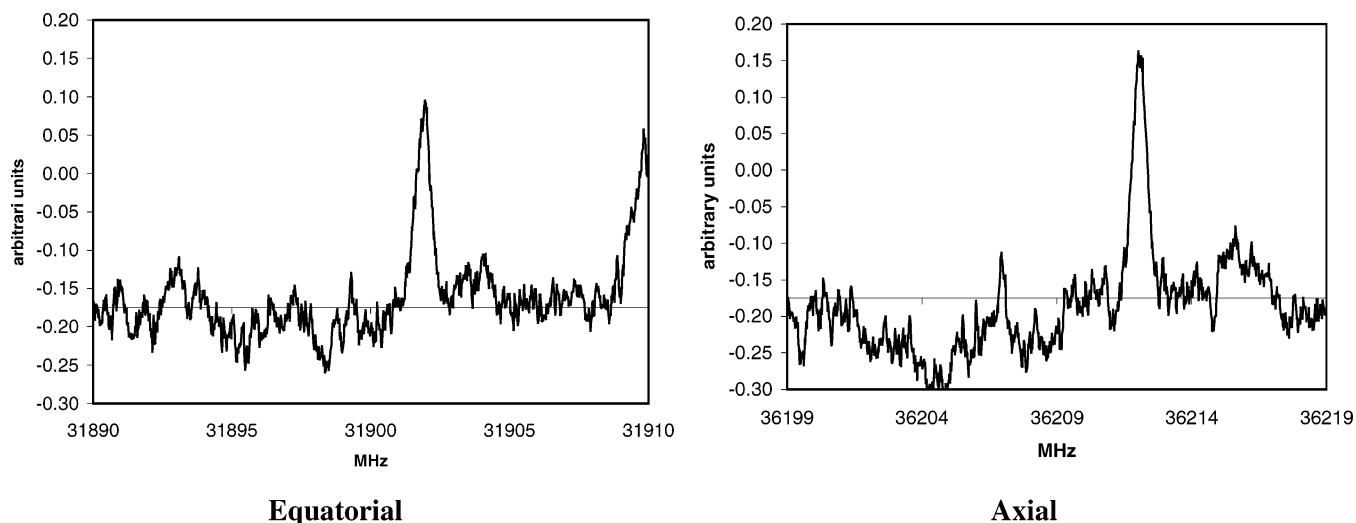


Figure 2. Rotational transition $10_{3,7} \leftarrow 9_{3,6}$ is shown for both conformers. That of the axial species appears slightly more intense.

TABLE 7: Stark Coefficients ($\text{Hz V}^{-2} \text{cm}^2$) and Dipole Moment Components (D) of Axial and Equatorial FSCH

dipole moments ^a	$J'(K'_a, K'_c) \leftarrow J''(K''_a, K''_c)$	M	$(\Delta\nu/E^2)_{\text{obs}}$	$(\Delta\nu/E^2)_{\text{calc}}$
	9(4,6) \leftarrow 8(4,7)	1	1.14 (9)	1.20
axial:		2	4.85 (10)	4.82
$ \mu_a = 1.48(2)$		3	10.97 (36)	10.84
$ \mu_c = 0.98(3)$	9(4,5) \leftarrow 8(4,6)	1	-0.98 (11)	-1.15
$ \mu_{\text{tot}} = 1.78(2)$	11(2,9) \leftarrow 10(2,8)	1	-2.13 (13)	-2.13
	8(3,5) \leftarrow 7(3,4)	1	-1.59 (5)	-1.50
equatorial:		2	-5.58 (20)	-5.80
$ \mu_a = 1.97(2)$		3	-12.96 (69)	-12.98
$ \mu_c = 0.00(4)$	9(2,7) \leftarrow 8(2,6)	1	-1.12 (17)	-1.00
$ \mu_{\text{tot}} = 1.97(2)$	10(2,8) \leftarrow 9(2,7)	1	0.71 (5)	0.80
	11(2,10) \leftarrow 10(2,9)	1	-2.35 (12)	-2.32

^a $\mu_b = 0$ by symmetry.

(6) Vibrational Satellites. Relative intensity measurements²³ of the rotational transitions of the vibrational satellites with respect to the ground state lead to an estimate of their vibrational energies, reported in Table 3.

One can obtain some more information on the nature of the corresponding vibrational modes from the changes of planar moments of inertia of the vibrational satellites with respect to the ground state. The planar moments of inertia (P_{gg} ; $g = a, b, c$) are defined and related to the rotational constants as $P_{\text{aa}} = \sum_i m_i a_i^2 = h/(16\pi^2) (-1/A + 1/B + 1/C)$, etc., and represent the mass extensions in the directions of the corresponding principal axis. The ΔP_{gg} 's are given at the bottom of Table 3. The values of ΔP_{aa} and of ΔP_{cc} are positive and negative, respectively for $\nu = 1$ of the axial form; the opposite is true for $\nu_1 = 1$ of the equatorial species. They most probably correspond to the vibrational motion which brings to the inter-conformational change. A shrinking of the molecule along the c -axis, and an elongation along the a -axis take place, indeed, in going from axial to equatorial, and vice versa.

Conclusions

The axial/equatorial conformational features of FSCH are quite different with respect to those of the cyclohexane homologue, fluorocyclohexane, being the axial form the slightly more stable. The experimental evidence is confirmed by the ab initio calculations.

Structural differences between the two conformers are found to be significant (quite larger than experimental uncertainties)

only for parameters α and β in Figure 1. In going from the axial to the equatorial form, α increases by 5° and β decreases by 4° . This may be an effect to reduce the larger steric hindrance, in the equatorial conformer, between the F atom and the adjacent axial hydrogens on C2 and C6. Such steric hindrance is less for the axial conformer because in this case the adjacent hydrogens are in an equatorial position.

Shifts of second moments of inertia in going from the ground to the excited state indicate that the vibrational satellite belongs to the deformation of the ring, which leads to the conformational interchange.

Acknowledgment. We thank Aldo Millemaggi for technical help. This work was supported by the University of Bologna, the Ministero dell'Università e della Ricerca Scientifica e Tecnologica and the Consiglio Nazionale delle Ricerche.

Supporting Information Available: Two tables of rotational transition frequencies. This material is available free of charge via the Internet at <http://pubs.acs.org>.

References and Notes

- (1) Bovey, F. A.; Hood, F. P.; Kornegay, R. L.; Anderson, E. W. *J. Chem. Phys.* **1964**, *40*, 3099.
- (2) Chu, P. S.; True, N. S. *J. Phys. Chem.* **1985**, *89*, 5613.
- (3) Pierce, L.; Nelson, R. *J. Am. Chem. Soc.* **1966**, *88*, 216. Pierce, L.; Beecher, J. F. *J. Am. Chem. Soc.* **1966**, *88*, 5406. Scharpe, L. H. *J. Am. Chem. Soc.* **1972**, *94*, 3737.
- (4) Fishman, A. I.; Herrebout, W. A.; van der Veken, B. J. *J. Phys. Chem. A* **2002**, *106*, 4536.
- (5) Christian, S. D.; Grundnes, J.; Klaeboe, P.; Torneng, E.; Woldbaek, T. *Acta Chem. Scand. A* **1980**, *34*, 391.
- (6) Damiani D.; Ferretti, L. *Chem. Phys. Lett.* **1973**, *21*, 592. Caminati, W.; Scappini, F.; Damiani, D. *J. Mol. Spectrosc.* **1984**, *108*, 287.
- (7) Atkinson, V. A. *Acta Chem. Scand.* **1961**, *15*, 599.
- (8) Fishman, A. I.; Klimovitskii, A. E.; Skvortsov, A. I. *J. Raman. Spectrosc.* **1997**, *28*, 623.
- (9) Allinger, N. L.; Liang, C. D. *J. Org. Chem.* **1967**, *32*, 2391.
- (10) Shen, Q.; Peloquin, J. M. *Acta Chem. Scand. A* **1988**, *42*, 367.
- (11) Holly, S.; Jalsovszky, G.; Egyed, O. *J. Mol. Struct.* **1982**, *79*, 465.
- (12) Woldbaek, T. *Acta Chem. Scand. A* **1982**, *36*, 641.
- (13) Damiani, D.; Scappini, F.; Caminati, W.; Corbelli, G. *J. Mol. Spectrosc.* **1983**, *100*, 36. Caminati, W.; Damiani, D.; Scappini, F. *J. Mol. Spectrosc.* **1984**, *104*, 183.
- (14) Abramczyk, H.; Barut, M.; Benaltabef, A.; Escribano, R. *Chem. Phys.* **1994**, *181*, 393.
- (15) Ekejiuba, I. O.; Hallam, H. E. *Spectrosc. Lett.* **1969**, *2*, 347.
- (16) Bushweller, C. H. In *Conformational Behavior of Six-Membered Rings*; Juaristi, E., Ed.; VCH Publishers: New York, 1995; pp 25–58.
- (17) Favero, L. B.; Caminati, W.; Árnason I.; Kvaran, Á. *J. Mol. Spectrosc.* **2005**, *229*, 188.

- (18) Arnason, I.; Kvaran, A.; Jonsdottir, S.; Gudnason, P. I.; Oberhammer, H. *J. Org. Chem.* **2002**, *67*, 3827.
- (19) Schott, V. G.; Schneider, P.; Kelling, H. *Z. Anorg. Allg. Chem.* **1973**, *398*, 293.
- (20) Arnason, I.; Kvaran, Á.; Jónsdóttir, S.; Bodi, A.; Belyakov, S.; Oberhammer, H. Manuscript in preparation.
- (21) Wodarczyk, F. J.; Wilson, E. B., Jr. *J. Mol. Spectrosc.* **1971**, *37*, 445.
- (22) Grabow, J.-U.; Stahl, W. *Z. Naturforsch. A* **1990**, *45*, 1043. Grabow, J.-U., Ph.D. Thesis, Kiel University, Germany, 1992.
- (23) Caminati, W.; Millemaggi, A.; Alonso, J. L.; Lesarri, A.; López, J. C.; Mata, S. *Chem. Phys. Lett.* **2004**, *392*, 1.
- (24) Frisch, M. J.; et al. *Gaussian 03*, revision B.04; Gaussian, Inc.: Pittsburgh, PA, 2003.
- (25) Watson, J. K. G. In *Vibrational Spectra and Structure*; Durig, J. R., Ed.; Elsevier: New York/Amsterdam, 1977; Vol. 6, pp 1–89.
- (26) Kraitchman, J. *Am. J. Phys.* **1953**, *21*, 17.
- (27) Curl, R. F. *J. Comput. Phys.* **1957**, *27*, 343.
- (28) Reinartz, I. M. L. J.; Dymanus, A. *Chem. Phys. Lett.* **1974**, *24*, 346.
- (29) Golden, S.; Wilson, E. B., Jr. *J. Chem. Phys.* **1948**, *24*, 669.
- (30) Esbitt, A. S.; Wilson, E. B., Jr. *Rev. Sci. Instrum.* **1963**, *34*, 901.